

## **Supplementary material**

### **Polycaprolactone enabled sealing and carbon composite electrode integration into electrochemical microfluidics**

Kevin J. Klunder,<sup>\*a,b</sup> Kaylee, Cynthia,<sup>a</sup> Kate berg,<sup>a</sup> Shelley D. Minteer,<sup>b</sup> and Charles S. Henry<sup>a</sup>

<sup>a</sup>Department of Chemistry, Colorado State University, Fort Collins, CO 80523

<sup>b</sup>Department of Chemistry, University of Utah, Salt Lake City, UT 84112

\*Corresponding author

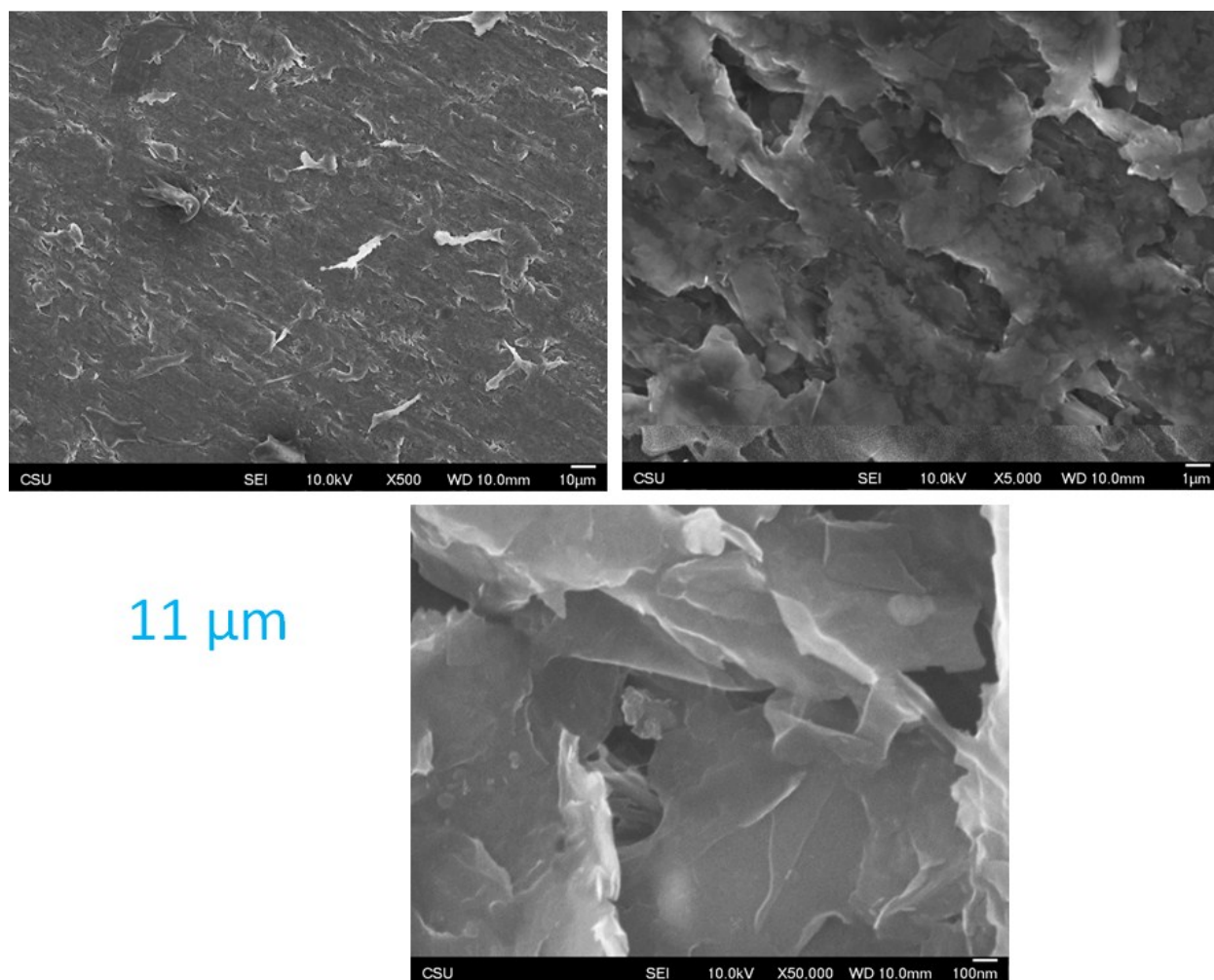


**Figure S1** SEM images of a 1:2 11 μm electrode

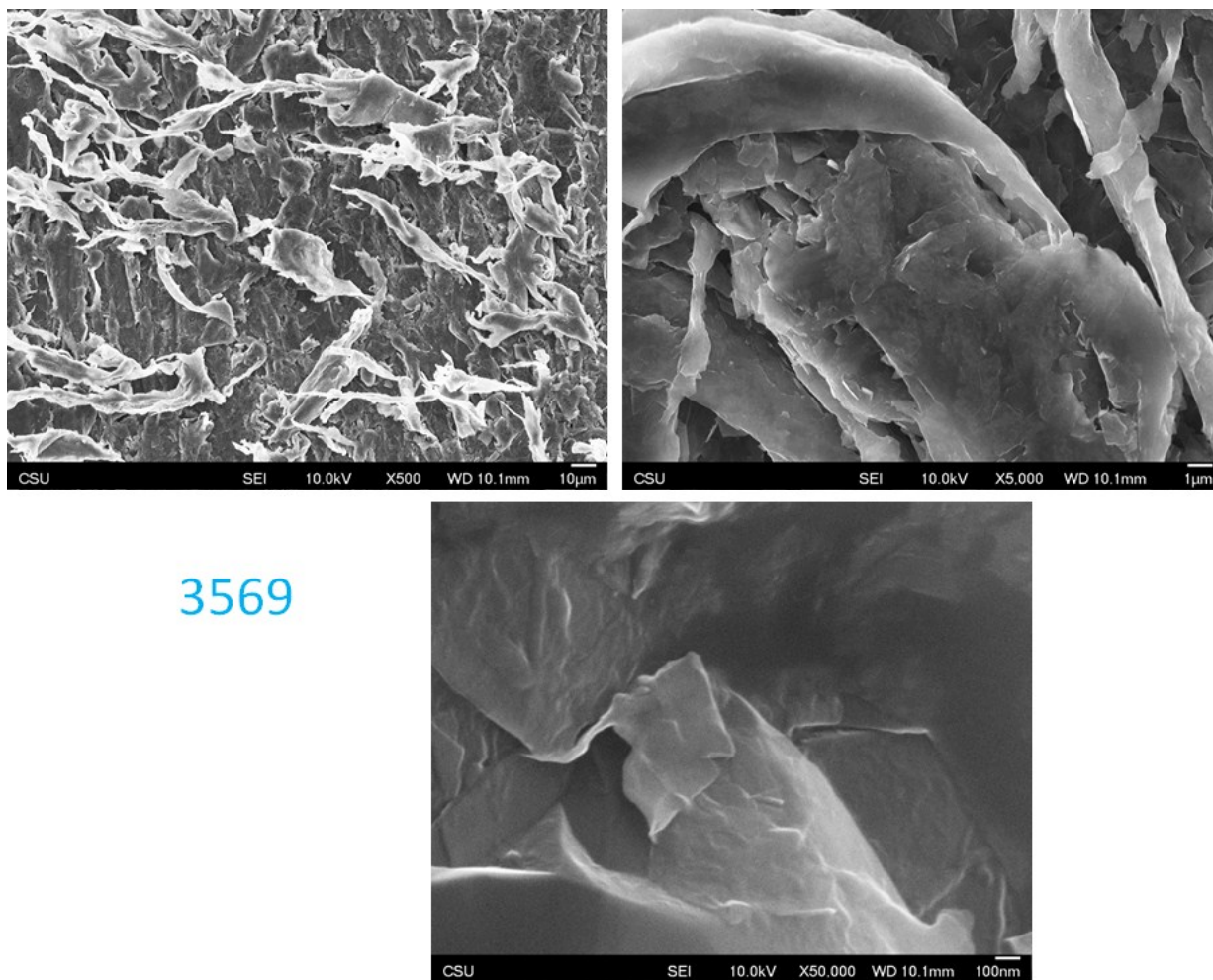


**Figure S2** SEM images of a 1:2 3569 electrode

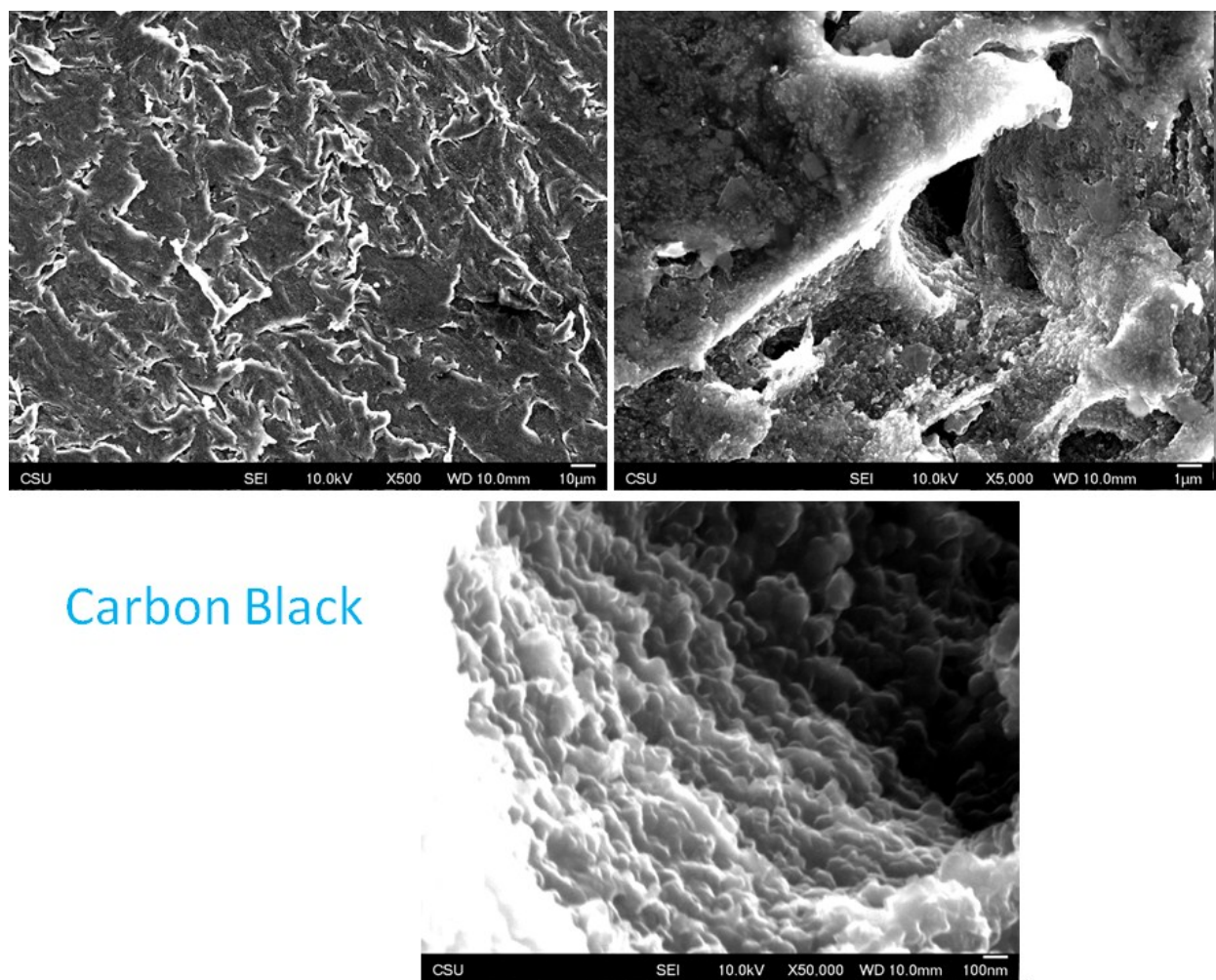


**Figure S3** SEM images of a 3:4 Carbon Black electrode

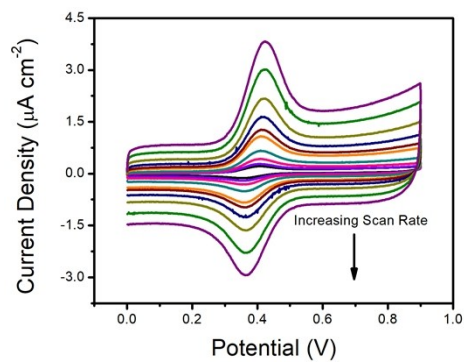


**Figure S4** Representative CV's for scan rate study for 1 mM FcTMA<sup>+</sup> in 0.5 M KNO<sub>3</sub> on 1:2 PCL:MG-1599 electrode ( $v = 25, 50, 100, 200, 400, 500, 700, 1000, 1500, 2000$  mV/s).

| Scan Rate<br>(mV/s) | $\Delta E$ (mV)         |                         |                 |                 |                    |                    |
|---------------------|-------------------------|-------------------------|-----------------|-----------------|--------------------|--------------------|
|                     | 1:2<br>PCL:11<br>micron | 1:4<br>PCL:11<br>micron | 1:2<br>PCL:3569 | 1:4<br>PCL:3569 | 1:2<br>PCL:MG-1599 | 1:4<br>PCL:MG-1599 |
| 25                  | 56 $\pm$ 5              | 54 $\pm$ 2              | 50 $\pm$ 5      | 53 $\pm$ 3      | 55 $\pm$ 8         | 57 $\pm$ 6         |
| 50                  | 53 $\pm$ 4              | 55 $\pm$ 0              | 53 $\pm$ 8      | 58 $\pm$ 8      | 53 $\pm$ 5         | 56 $\pm$ 4         |
| 100                 | 56 $\pm$ 2              | 52 $\pm$ 6              | 53 $\pm$ 5      | 56 $\pm$ 1      | 46 $\pm$ 2         | 51 $\pm$ 5         |
| 200                 | 49 $\pm$ 2              | 52 $\pm$ 3              | 52 $\pm$ 9      | 54 $\pm$ 3      | 47 $\pm$ 3         | 51 $\pm$ 5         |
| 400                 | 54 $\pm$ 5              | 57 $\pm$ 4              | 51 $\pm$ 10     | 54 $\pm$ 4      | 55 $\pm$ 5         | 56 $\pm$ 2         |
| 500                 | 55 $\pm$ 3              | 58 $\pm$ 4              | 54 $\pm$ 10     | 59 $\pm$ 2      | 56 $\pm$ 3         | 59 $\pm$ 1         |
| 700                 | 56 $\pm$ 7              | 59 $\pm$ 1              | 51 $\pm$ 2      | 59 $\pm$ 2      | 55 $\pm$ 6         | 59 $\pm$ 1         |
| 1000                | 63 $\pm$ 3              | 64 $\pm$ 4              | 59 $\pm$ 5      | 59 $\pm$ 4      | 56 $\pm$ 4         | 60 $\pm$ 2         |
| 1500                | 61 $\pm$ 3              | 70 $\pm$ 1              | 61 $\pm$ 6      | 67 $\pm$ 1      | 55 $\pm$ 3         | 65 $\pm$ 2         |
| 2000                | 61 $\pm$ 1              | 70 $\pm$ 3              | 70 $\pm$ 4      | 64 $\pm$ 3      | 58 $\pm$ 1         | 66 $\pm$ 4         |

**Table S1** Scan rate study for 1 mM FcTMA<sup>+</sup> in 0.5 M KNO<sub>3</sub>, error from standard deviation of 3 different electrodes.

| Scan Rate<br>(mV/s) | $\Delta E$ (mV)         |                         |                 |                 |                    |                    |
|---------------------|-------------------------|-------------------------|-----------------|-----------------|--------------------|--------------------|
|                     | 1:2<br>PCL:11<br>micron | 1:4<br>PCL:11<br>micron | 1:2<br>PCL:3569 | 1:4<br>PCL:3569 | 1:2<br>PCL:MG-1599 | 1:4<br>PCL:MG-1599 |
| 25                  | 72 $\pm$ 5              | 74 $\pm$ 4              | 77 $\pm$ 7      | 69 $\pm$ 2      | 75 $\pm$ 2         | 75 $\pm$ 7         |
| 50                  | 79 $\pm$ 7              | 76 $\pm$ 6              | 81 $\pm$ 8      | 73 $\pm$ 2      | 79 $\pm$ 3         | 79 $\pm$ 5         |
| 100                 | 85 $\pm$ 6              | 81 $\pm$ 5              | 88 $\pm$ 11     | 77 $\pm$ 2      | 84 $\pm$ 3         | 88 $\pm$ 6         |
| 200                 | 95 $\pm$ 6              | 86 $\pm$ 8              | 94 $\pm$ 14     | 83 $\pm$ 6      | 95 $\pm$ 5         | 98 $\pm$ 10        |
| 400                 | 107 $\pm$ 10            | 100 $\pm$ 8             | 103 $\pm$ 13    | 93 $\pm$ 6      | 106 $\pm$ 7        | 116 $\pm$ 10       |
| 500                 | 115 $\pm$ 9             | 103 $\pm$ 10            | 107 $\pm$ 13    | 97 $\pm$ 8      | 111 $\pm$ 10       | 119 $\pm$ 12       |
| 700                 | 121 $\pm$ 5             | 108 $\pm$ 7             | 111 $\pm$ 13    | 101 $\pm$ 9     | 119 $\pm$ 9        | 127 $\pm$ 13       |
| 1000                | 131 $\pm$ 8             | 119 $\pm$ 8             | 110 $\pm$ 13    | 108 $\pm$ 10    | 128 $\pm$ 9        | 140 $\pm$ 15       |
| 1500                | 136 $\pm$ 11            | 131 $\pm$ 6             | 116 $\pm$ 9     | 115 $\pm$ 15    | 132 $\pm$ 8        | 155 $\pm$ 19       |
| 2000                | 142 $\pm$ 10            | 143 $\pm$ 9             | 124 $\pm$ 11    | 119 $\pm$ 19    | 135 $\pm$ 9        | 163 $\pm$ 17       |

**Table S2** Scan rate study for 5 mM ferri/ferrocyanide in 0.5 M KNO<sub>3</sub>, error from standard deviation of 3 different electrodes.

The heterogeneous electron transfer rate constants ( $k^0$ ) were calculated using the Nicholson method.<sup>40</sup> The following equation was used:

$$\psi = k^0[\pi D n F \nu / RT]^{-1/2}$$

The kinetic parameters ( $\psi$ ) from the average  $\Delta E$ s of the ferri/ferrocyanide peaks for each scan rate were plotted versus  $[\pi D n F \nu / RT]^{-1/2}$  where  $D$  is the diffusion coefficient,  $F$  is Farady's constant,  $\nu$  is the scan rate,  $R$  is the ideal gas constant, and  $T$  is temperature. The rate constants

were determined from the slopes of the regression lines and the error shown is the standard error of the slope.

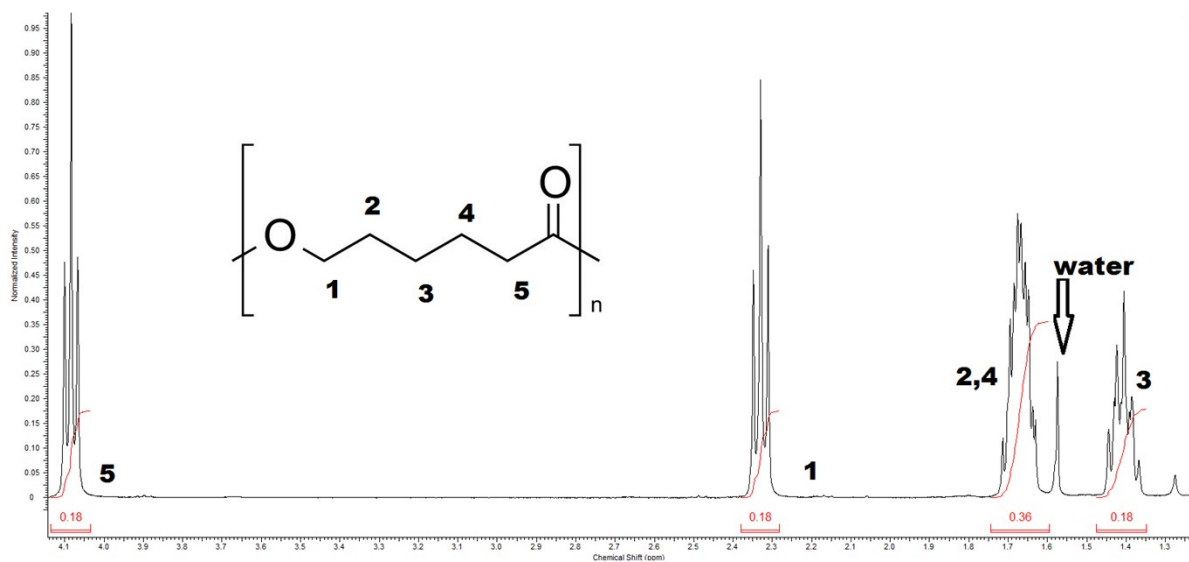


**Figure S5** <sup>1</sup>H-NMR spectra of ThermoMorph polymer in CDCl<sub>3</sub>.



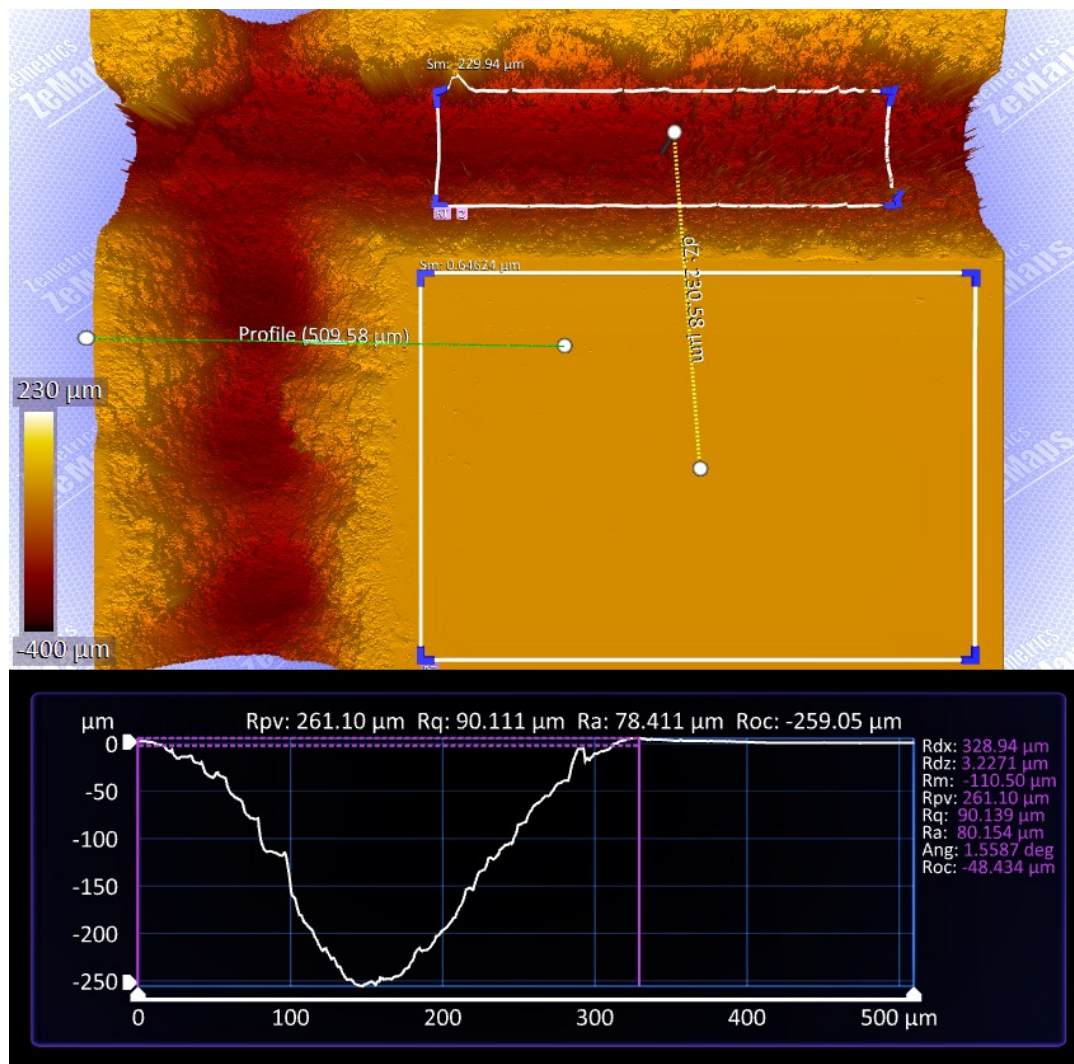


**Figure S6** Optical profilometry of a channel cut into a droplet generator of a single pass in the X-axis of the laser cutter.

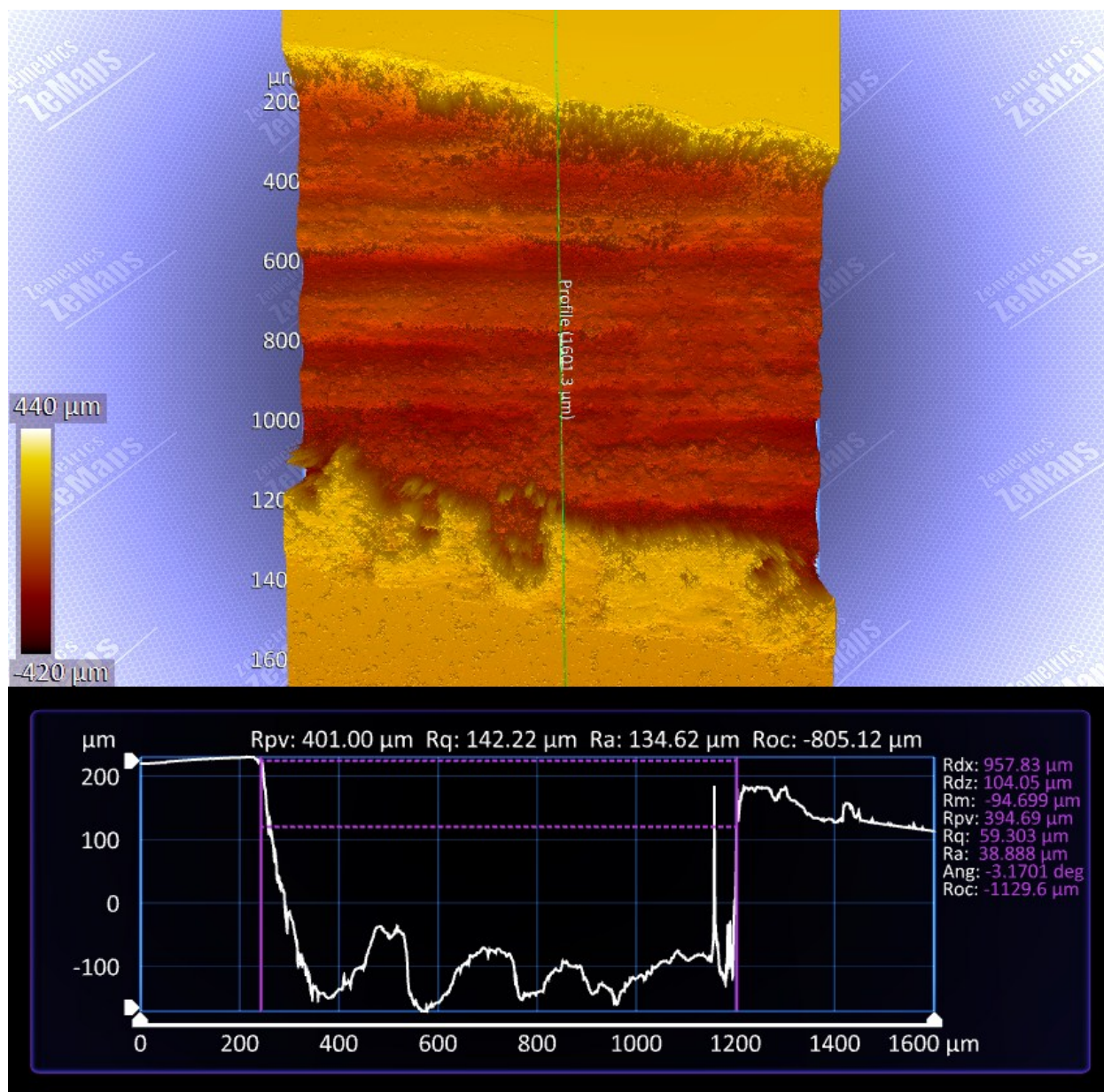


**Figure S7** optical profilometry of a channel cut into a droplet generator of a single pass in the Y-axis of the laser cutter. Image is of the waste zone of the droplet generator.



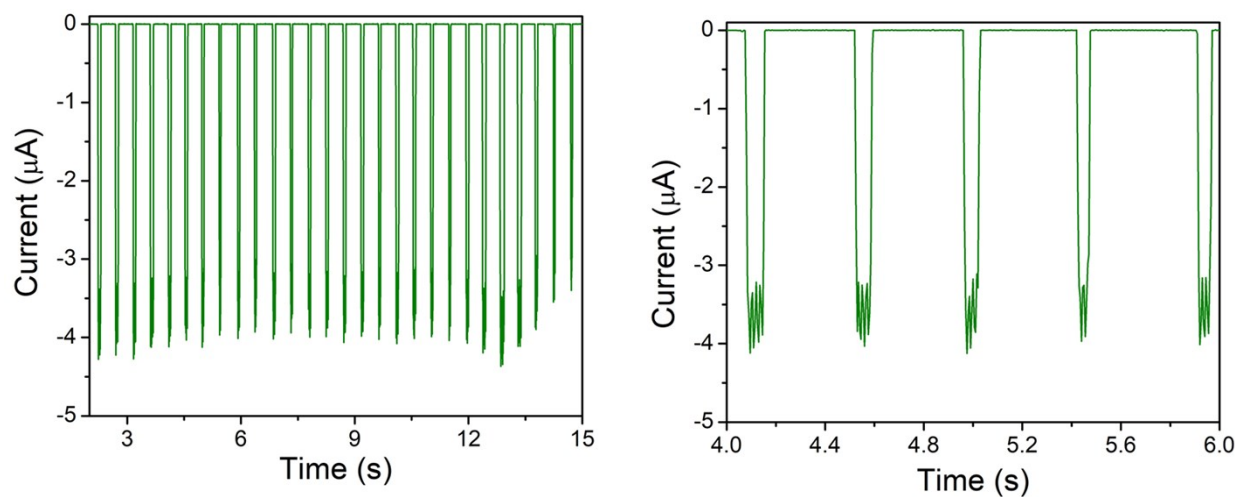


**Figure S8** Droplet generation in a salinized microfluidic chip, demonstration of short term stability for the sending of water droplets. Droplets contained 1 mM of ferricyanide in 0.5 M KCl.

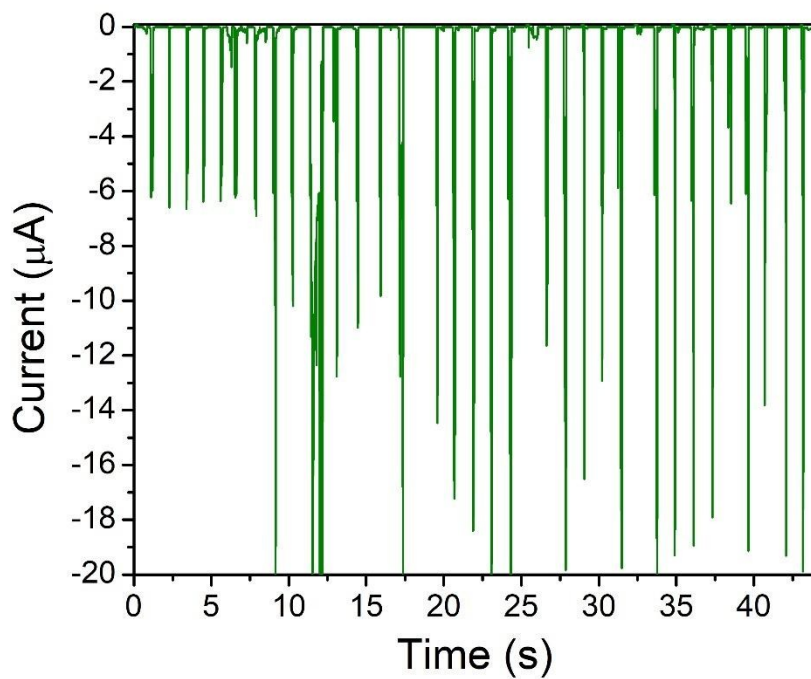


**Figure S9** Droplet generation in a salinized microfluidic chip, demonstrating instabilities in droplet sensing in a second run. Droplets contained 1 mM of ferricyanide in 0.5 M KCl.